

A Study of the Parameters Affecting Minimum Detectable Activity Concentration Level of Clinical LSO PET Scanners

Nicolas A. Karakatsanis, *Student Member, IEEE*, Konstantina S. Nikita, *Senior Member, IEEE*

Abstract— Recent studies in the field of molecular imaging have demonstrated the need for PET imaging probes capable of imaging very weak activity distributions. Over this range of applications the sensitivity and the energy resolution of a PET system can be critical, as it can possibly affect the minimum amount of activity which can be reliably detected. Clinical PET systems, as opposed to small animal systems, are less sensitive and, therefore, imaging of very low activity sources could be challenging. Moreover the presence of LSO crystal detectors can further raise the minimum detection threshold due to the intrinsic radioactivity of the ^{176}Lu contained in the LSO compound. Our aim is to examine the feasibility of using an LSO-based clinical PET scanner for imaging activity distributions of 4nCi/mm^3 or less. In this study the parameter of minimum detectable activity (MDA) has been used for the quantification of the detection threshold of a system. A series of acquisitions was simulated using the Monte Carlo simulation software package of GATE. Existing validated GATE models of the clinical Siemens Biograph 6 PET/CT and pre-clinical microPET Focus 220 scanners have been applied to quantify and compare the effect of the LSO background and the energy window on the MDA performance of the systems. Four square regions, each with a unique signal-to-background activity concentration ratio (SBR), were scanned simultaneously. The intrinsic LSO background spectrum and the total energy spectrum, as well as their relative positions and intensities were estimated. The simulated data were histogrammed on various time frames, which were later reconstructed using a filtered back-projection algorithm. Detectability in every image was quantified using a modified Currie equation to associate an MDA value with a specific region and frame length. In the case of Biograph an MDA of 4nCi/mm^3 can be reliably detected for frame lengths longer than 5min and in regions where the SBR was higher than 4. When higher contrast regions are imaged, detection can be achieved even for frame lengths down to 1min. The previous analysis was repeated by using a GATE model of a hypothetical BGO-based clinical PET scanner. The results between the two scanner models were compared with each other as well as with those of a previous MDA study on a pre-clinical microPET Focus 220 scanner.

I. INTRODUCTION

A significant number of clinical Positron Emission Tomography (PET) imaging systems developed the last decade are equipped with lutetium oxyorthosilicate (LSO) scintillating crystal detectors. LSO has been established as

the crystal of choice for PET imaging due to its highly efficient stopping power and light yield and its short decay time. However LSO crystals contain by 20% the natural radioactive element of ^{176}Lu with a very long half-life, on the order of 1010 years, causing the contamination of the total true energy spectrum of each scan performed. We measured the total LSO intrinsic radioactivity for the Siemens Biograph 6 LSO scanner to be approximately 79uCi . Therefore its effect on the detectability of the Biograph scanner should be minor, when activity distributions with total activity on the order of mCi are imaged. In this case, the LSO background would be negligible, comparing to the total activity present, as it is distributed evenly across the entire field of view of the scanner.

However, an increasing number of recent molecular imaging studies have brought the need to image source distributions of very low activity concentration, such as below 10nCi/mm^3 . In this range of concentrations the sensitivity of the imaging system plays an important role, as it determines the minimum amount of activity that can be reliably detected. Clinical PET systems, as opposed to pre-clinical, are characterized by a relative low sensitivity and therefore the detection of very low concentrations could be a challenging task. Obviously, the detection threshold for a particular target is depending on the activity concentration level of the surrounding background activity distribution. Moreover the presence of LSO crystal detectors will result in an additional ^{176}Lu -induced background activity that will raise the detection threshold further. In this study we are examining the feasibility of using an existing clinical PET system, designed originally for clinical studies with relative high activity concentration, to perform imaging studies of less than 10nCi/mm^3 . In order to evaluate the ability of an imaging system to detect very weak source distributions we will introduce the performance parameter of minimum detectable activity or MDA.

The MDA will be defined here as the minimum mean number of net signal counts per reconstructed voxel that are required to yield a reconstructed image, where the probability of having false-positive for higher number of counts or false-negative detection for lower number of counts is in both cases 5% or less. The MDA value, as defined above, determines a lower threshold for the detected net signal counts which corresponds to a specific activity concentration for the signal distribution examined. The Currie equation (1) provides a generalized estimate of the MDA which is proportional to the standard deviation of the

Manuscript received July 5th, 2008.

This work was supported by the Greek Secretariat of Research and Technology (GSRT) project Greece-USA collaborations, under grant 05-NONEU-69

N. A. Karakatsanis and K. S. Nikita are with the Department of Electrical and Computer Engineer, Biomedical Simulations and Imaging Laboratory of the National Technical University of Athens, 9 Iroon Polutechniou St., 15780, Athens, GR (e-mail: knicolas@mail.ntua.gr).

background counts σ_{bkgrd} at a specific Volume of Interest (VOI) [1].

$$MDA = 4.653\sigma_{\text{bkgrd}} + 2.706 \quad (1)$$

Currie equation (1) sets detection limit assuming Poisson distribution with noise in the measurement of both the total and background counts. The background counts include all the counts induced by all other sources of activity except from the signal source, whereas the net counts can be calculated by subtracting the background counts from the total counts.

In the case of LSO-based PET scanners the non-negligible background counts originating from the intrinsic radioactivity of ^{176}Lu raise the detection limit as follows:

$$MDA = 4.653\sqrt{\sigma_{\text{bkgrd}}^2 + \sigma_{\text{LSO}}^2} + 2.706 \quad (2)$$

where σ_{bkgrd} is the standard deviation of the LSO background counts. Because we assume Poisson distribution for the background and LSO counts, MDA can be calculated as follows

$$MDA = 4.653\sqrt{N_{\text{bkgrd}}^2 + N_{\text{LSO}}^2} + 2.706 \quad (3)$$

where N_{bkgrd} and N_{LSO} are the background and LSO detected counts.

According to the decay scheme of ^{176}Lu β - particles (420keV) are emitted in cascade with γ photons of energies of 307keV (94%), 202keV (78%) and 88keV (15%) [2]. Therefore if the energy window of the PET scanner is chosen large enough to include at least one of the three previously mentioned gamma energy peaks, random coincidences between the gamma photons of the true annihilation events and the gamma photons induced by ^{176}Lu decay can take place, affecting prompt coincidences when source distributions of very low activity concentration are scanned and possibly resulting in significant artifacts at the final reconstructed image. Consequently, the detectability of point sources within a uniform background activity region can be also adversely affected in the presence of LSO. [3-5]

Our purpose in this study is to assess the MDA value of the clinical LSO-based Siemens Biograph 6 PET scanner by using a validated model of the scanner and simulating various point-like signal activity distributions, lower than 5nCi/mm^3 , that are surrounded by uniform background activity regions for different acquisition lengths.

II. MATERIALS AND METHODS

In this study we have used Geant4 Application for Tomography Emission (GATE) in order to model the PET function component of a Siemens Biograph 6 PET/CT clinical scanner. GATE is a simulation package, based on the well-validated Geant4 simulation software, specially designed for nuclear medicine applications and supported by a large community of developers and users [6]. It's capability to efficiently model the simultaneous radioactive decay of multiple isotopes in the same FOV in the course of time, as well as it's flexibility in setting various digitizer

parameters of it's imaging systems model, such as the energy window, were the reasons we selected GATE as our simulation tool for this study. Moreover GATE allowed us to accurately reproduce acquisition time lengths and customized activity distributions with specific concentration values that have been previously used for similar MDA studies in small animal PET systems. Thus, it became possible to apply a standardized method in order to comparatively evaluate the MDA performance of clinical and pre-clinical PET imaging systems.

In this work we have applied the GATE model of the Siemens Biograph 6 PET/CT clinical system, which has already been validated for its performance parameters of sensitivity, scatter fraction and spatial resolution [7],[8]. The ^{176}Lu radioactive source was simulated by employing the Geant4 ion source model and confining it to the entire detector volume of the scanner.

The activity distributions modeled in this study are similar to those that have been used in the study of the assessment of the MDA value for the pre-clinical small animal microPET Focus 220 scanner [9]. GATE source geometry consists here of four papers, each in transaxial orientation, placed along the axis of the detector rings, perpendicular to the scanner bed. The thickness of the papers was 0.16mm while the axial distance between two neighboring papers was set to 10.4mm.

On each paper we simulated a $45 \times 45 \text{mm}^2$ printed uniform signal background activity distribution of constant activity, as well as a $2 \times 2 \text{mm}^2$ printed signal distribution of varying activity level. The signal distribution was placed on top of the signal background at the center of the lower left part of its distribution, as in the pre-clinical scanner study. The background source distributions were modeled with approximately the same activity concentration value for all four papers, whereas the source distributions varied accordingly, so as to ensure the formation of four different regions, corresponding to one of the four papers, in terms of signal-to-background activity concentration ratio (SBR). All the activity concentration values Because of the relative differences between the detector rings of the microPET Focus 220 and the Biograph 6, the activity distributions in the second case were 9 times larger in size. The total activity was set accordingly in order to preserve the same activity concentration values for both the signal and the background regions in both studies. Consequently, each of the four regions was characterized by an identical SBR in both studies.

In this work we are interested in assessing the ability of the imaging system to accurately count a target distribution without taking into account partial volume effects and interactions between signal and background voxels in the final reconstructed image. Therefore the signal source was modeled as a point-like activity distribution with dimensions smaller than the measured spatial resolution of the system. The GATE material definition of water was chosen to model the surrounding water-equivalent material that had been used

in the preclinical study to ensure annihilation of emitted positrons. The geometry of the GATE simulation is presented in Fig. 1. This configuration allowed the simultaneous data acquisition from all four different signal-to-background contrast regions

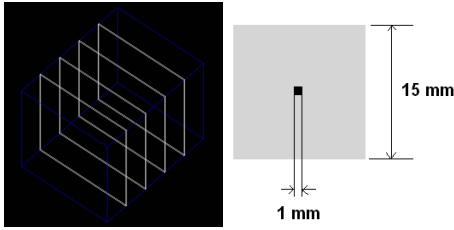


Fig.1. Geometric configuration of the four plane activity distributions in a transaxial orientation along the axis of the scanner (left) and relative position and dimensions of the printed point source and the background source (right)

In order to calculate the SBR value for each of the four contrast regions in this study we designed two regions of interest (ROIs) in the reconstructed image, the signal and background ROI, each corresponding to the target point source and the surrounding background area respectively. Since the point source distribution of the signal is placed on top of the background distribution, the mean number of activity concentration measured within the signal ROI is the sum of the mean signal and background concentration. Therefore the SBR for each region is calculated by taking the ratio of the above sum to the measured background activity distribution. The simulated activity concentration for the four point sources starting from the highest-contrast region is approximately 4, 3, 2 and 1nCi/mm³, whereas the background activity concentration was set to approximately 330pCi/mm³ for all contrast regions. The calculated SBR values for each region are presented at Table I, together with the IDs of each region.

TABLE I
SIGNAL TO BACKGROUND ACTIVITY CONCENTRATION RATIOS

Region Type ¹	A	B	C	D
Signal to Background Ratio	6.7	5.3	4.5	2.9

¹Each region is identified by a type (A, B, C or D), which is associated with a signal to background activity concentration ratio.

A data acquisition of 15min was simulated with GATE using the medium energy window of 400-650keV, which is the standard window of Biograph applied for most clinical imaging studies. This window is expected to reject most of the random events induced by the intrinsic LSO background, since it excludes and the three gamma energy peaks of the ¹⁷⁶Lu emission spectrum, and therefore improve the scanner sensitivity. The data was histogrammed in time frames of 30sec, 1min, 2min, 5min, 10min and 15min. These

acquisition times are common for molecular imaging applications and preclinical studies and were selected to examine the feasibility of performing similar studies using a commercial clinical PET imaging system.

A FBP-3D re-projection algorithm, implemented in STIR software package, was applied to the projection data and the reconstructed images were later analyzed to estimate the MDA value for each region as a function of the frame length [10].

In this particular study the point source signal is of much less intensity comparing to the respective background activity, allowing us to consider that its contribution to the minimum detectable activity calculation is negligible and, therefore the constant term of Currie equation can be ignored (1) resulting in the following modified Currie equation which implies a lower MDA threshold for the system [1]

$$MDA = 4.653 \sqrt{N_{bkg}^2 + N_{LSO}^2} \quad (4)$$

In order to quantify the image data we drew an ROI at each of the four point sources and a relatively larger ROI at the background of each region. The maximum signal pixel value and background standard deviation were measured.

The mean pixel value of the background ROI was subtracted from the maximum pixel value of the respective signal ROI to estimate the maximum net signal counts. The measured total background standard deviation was used to calculate the MDA value according to Eq. (3). Finally the ratio of the maximum net signal counts to the MDA value was calculated to decide whether the measured number of counts in a signal ROI came from the actual point source or the background. If the ratio is higher than unity, then we can claim with an uncertainty of 5% or less that a real signal was detected by the PET imaging system and signal activity was indeed present within this ROI.

Furthermore we applied GATE in order to determine the energy spectrum of the intrinsic LSO background singles and coincidences. The respective contribution of the scintillator background to the total energy spectrum when the four background and four signal sources are present in the FOV was also determined. The geometry set-up of this GATE simulation is depicted at figure 2.

Subsequently a new GATE model was designed after replacing the LSO with BGO detectors and the previous MDA quantification analysis for the 4 contrast regions was repeated. The new simulated results were compared with the previous and the effect of the intrinsic LSO radioactivity to the MDA performance parameter of a clinical system was determined.

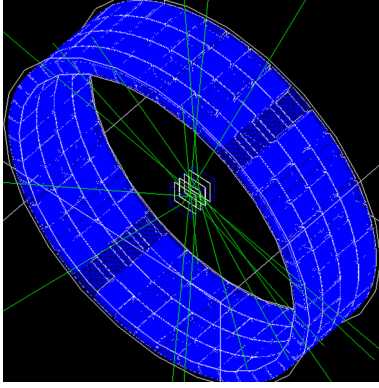


Fig.2. Geometric configuration of the four plane activity distributions in a transaxial orientation along the axis of the scanner (left) and relative position and dimensions of the printed point source and the background source (right)

III. RESULTS AND DISCUSSIONS

A. Characteristics of LSO background intrinsic activity

The singles and the coincidence energy spectrum of the LSO intrinsic background activity of a Biograph PET scanner are presented as diagrams, filled with blue color, at Fig. 4. Moreover the total singles and coincidence energy spectrum of a simulated 1min data acquisition of the four activity distributions are depicted with red lines at the same figure.

The ^{176}Lu energy spectrum contribution to the total singles energy spectrum is significant. However most of the ^{176}Lu induced events are rejected when coincidence sorting takes place because of the higher value of the low energy level discriminator (400keV) of the energy window applied, compared to the higher peak of the ^{176}Lu emission spectrum. However because of the 14% of energy resolution of the system a few LSO background coincidences were detected induced by the simultaneous detection of gamma particles of 307keV energy and emitted beta particles. The analysis of the simulated data has confirmed the beta-gamma coincidences by showing that the numbers of beta and gamma particles that resulted in coincidences were very similar.

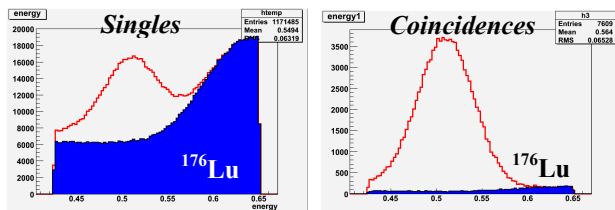


Fig. 4. Singles (left) and coincidences (right) energy spectrum. Total singles or coincidences energy spectrum (red line) and singles or coincidences energy spectrum of the ^{176}Lu intrinsic activity (curve filled with blue color). An typical energy window of 400-650keV has been used.

B. Performance analysis of microPET Focus 220 based on Minimum Detectable Activity parameter

The reconstructed images for 15min, 10min, 5min and 1min acquisition frames obtained from the simulated projection data for the case of the LSO-based Biograph scanner are presented in Fig. 5. Each frame consists of four different contrast regions. The measured signal to background ratio for each is given at Table I.

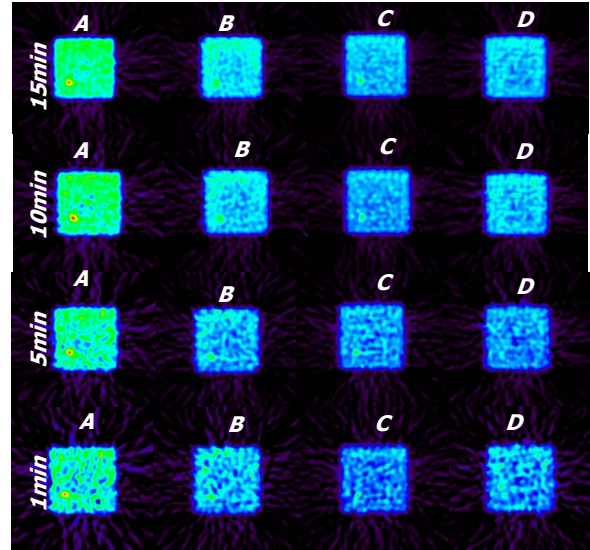


Fig. 5. Image data corresponding to the LSO-based Biograph GATE model. The simulated projection data were histogrammed into time frames of 15min, 10min, 5min and 1min respectively and reconstructed using FBP-3DRPJ algorithm of STIR package. Each frame consists of 4 different signal to background ratio regions, beginning at left with the highest ratio (region A) and ending to the right with the lowest ratio region (region D)

The equivalent images obtained from simulated projection data when the LSO detectors are replaced by BGO, are shown at Fig. 6.

Visual observation of the simulated reconstructed data indicates that a point source over a background activity distribution can be detected from the Biograph LSO scanner when data is acquired for at least 15min and the signal to background ratio (SBR) is higher or equal to 2.9, (region D). Moreover if the SBR of the imaging distribution is higher (region C) the acquisition length can be reduced down to 5min. Finally if the SBR is 6.7, equivalent to region A, or higher, then 1min acquisitions should be adequate for detection of the point source from the background activity.

The simulated data corresponding to the hypothetical scenario where Biograph is equipped with BGO detectors follow a similar trend, except from the MDA values measured at region D. We observe a slightly better detection limit for this region comparing to the LSO-based scanner. In this case the minimum acquisition length required to image point source distributions with SBR higher or equal to 2.9 is dropped down to 10min. The rest of the regions do not

appear to have any major visible discrepancies between the two cases for all the acquisition frame lengths. For both scanner configurations when 1min data acquisition was performed only the point source at region A could be clearly resolved. When viewing shorter time frames the statistical and image quality drops critically even for high-contrast regions such as region A.

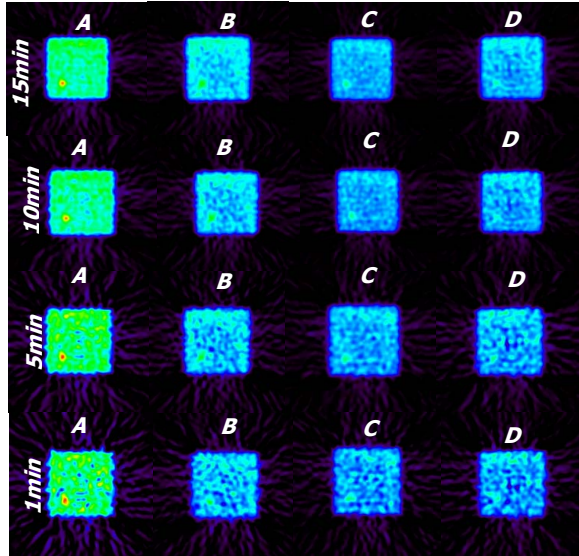


Fig. 6. Equivalent image data corresponding to the hypothetical model of Biograph when LSO detectors are replaced with BGO detectors. The same ramp filter settings as in the previous study were used for the reconstruction of the projection data

Certain artifacts and discrepancies can be observed in the above reconstructed images of both studies, which, however, are not critical for this study. The observation that most of these artifacts appear in both cases implies that they are not caused by the presence of LSO intrinsic radioactivity and are rather explained by the lack of normalization and attenuation correction on the projection data. These correction methods were not considered necessary for this work where small activity and attenuation distributions are used. However we believe that after a suitable normalization correction on the projection data, the reconstructed images will become smoother with more uniform activity distributions which could further improve the MDA performance.

Because of the uncertainty introduced by visualization, we use the MDA parameter as defined by Eq. (4) to quantify the ability of this LSO-based clinical scanner to reliably detect point-like activity distributions surrounded by a uniform background region, for different signal to background ratios and acquisition times. This quantification also provides a standard method to comparatively evaluate the MDA performance between LSO-based clinical systems and preclinical systems or hypothetical BGO-based clinical systems.

Following the ROI quantification analysis, Fig. 7 shows the data points that represent the ratio of the maximum net counts detected at a pixel of a signal ROI to the MDA value

for all four regions and for acquisition frames of 15min, 10min, 2min, 1min and 30sec in the case of the LSO-based simulated Biograph scanner. If the ratio is higher than unity, the detectability condition imposed by the Currie equation is satisfied and our point source distribution is considered to be detected with a 5% error probability [1].

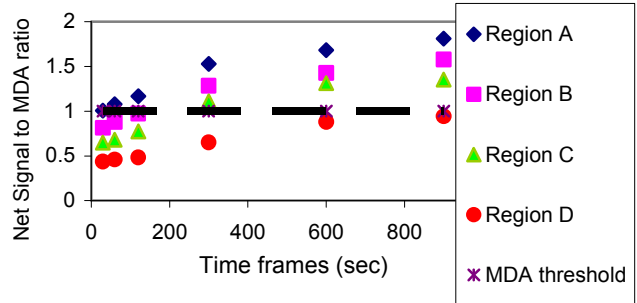


Fig. 7. Net signal counts to MDA value ratio for the simulated data of LSO-based Biograph as a function of different time frame durations and for different signal to background regions.

This quantification analysis was repeated for the GATE model of a hypothetical BGO-based clinical scanner as well and the results are presented at Fig. 8.

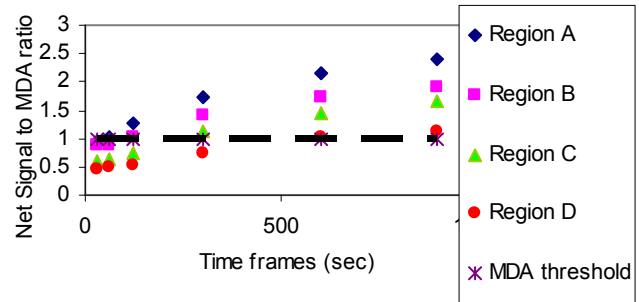


Fig. 8. Net signal counts to MDA value ratio for the simulated data of a hypothetical BGO-based clinical scanner as a function of different time frame durations and for different signal to background regions.

Moreover the respective quantification results for the case of the microPET Focus 220 scanner are included below for direct comparison of the detectability of clinical and pre-clinical PET imaging systems[9].

Based on the data points of Fig. 7 we come to the conclusion that the Biograph scanner can reliably count very weak point sources of approximately 4nCi/mm³ concentration within a uniform background, if the frame length is 5min or longer and the SBR is equal or higher than 4.5. This range of values is satisfied by regions A, B and C. However, if our SBR value is improved to 5.3 or higher, equivalent to region A and B, then a frame length of 1min is adequate to ensure detectability of the target point source.

In the case of a BGO-based PET clinical imaging system, we obtain a higher ratio for all regions, especially when the acquisition lasts for 5min or higher. However, the rise of the ratio do not appear to affect the decision to accept a count number as a reliable signal detection or to reject it as a false-positive, except from the case of the low-contrast region D

with a SBR value of 2.9. In the absence of LSO a frame length of 15min or higher now allows us to detect point-like activity distribution with a relative low contrast of 2.9. Therefore the removal of LSO background enhances the MDA performance of a clinical scanner but not to an extent where significant improvement can be observed.

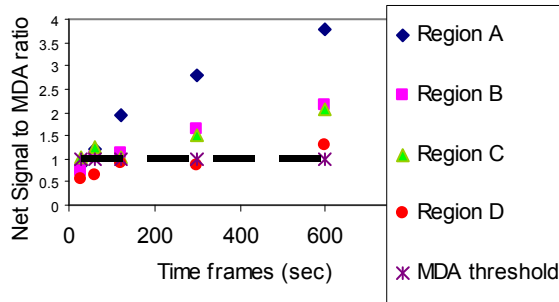


Fig. 9. Net signal counts to MDA value ratio for the simulated data of a microPET Focus 220 preclinical scanner as a function of different time frame durations and for different signal to background regions. This results have been validated with experimental measurements in a previous study.

A direct comparison between the MDA ratios achieved in a clinical and a pre-clinical scanner lead us to the conclusion that a better MDA ratio is calculated for all regions for the small animal scanner [9]. This result is expected because of the higher sensitivity of the small animal scanners due to their smaller size geometry. However, in all of the three cases, if a decision problem of acceptance or rejection of a measured count was applied, the outcome would be very similar, implying no major differences between the MDA performances of the three imaging systems. In particular, a great resemblance is observed between the MDA ratios of a BGO-based clinical system and a LSO-based small animal scanner. A careful observation of the MDA analysis data for all cases shows a relative high degree of uncertainty for frame lengths of 1min or shorter. In addition to the lack of normalization and attenuation correction, this uncertainty derives from the possible relative differences of the position of the signal and background ROIs in every region and histogrammed frame. Nevertheless these differences do not appear to affect the outcome of the MDA quantification analysis.

IV. CONCLUSIONS

In this study it was shown that very weak sources with activity concentration of 4nCi/mm³ can be reliably detected by the Biograph 6 LSO PET/CT system when the standard energy window of 400-650keV is applied.

Moreover, the LSO intrinsic radioactivity has only a minor effect on the detectability of low activity concentrations when the above energy window is applied. Therefore, replacement of the LSO detectors with BGO ones induced only a minor improvement of the MDA performance. Furthermore the comparative evaluation of the MDA, between all clinical and preclinical PET systems examined in this work, indicate similar performance in all

cases. However, small animal systems tend to have a slightly better detection limit [9]. In general, longer acquisition times or higher SBRs should lead to lower detection thresholds.

The conclusions of this work are useful for the design and validation of new PET clinical data acquisition protocols that will be applied to molecular imaging studies where very low amounts of activity is present. The optimal combination of signal-to-background activity concentration ratio and acquisition frame length can be determined from these protocols, allowing maximal sensitivity when very weak source distributions are imaged with clinical PET systems.

ACKNOWLEDGMENT

The authors would like to thank the OpenGATE collaboration for allowing us to use the GATE simulation software for the purposes of this study.

REFERENCES

- [1] L.A. Curie, "Limits for Qualitative Detection and Quantitative Determination" Application to Radiochemistry. *Analytical Chemistry* 40(3):586-593;1968
- [2] A. L. Goertzen, J. Y. Suk, C. J. Thompson, "Imaging of Weak-Source Distributions in LSO-Based Small-Animal PET Scanners", *Journal of Nuclear Medicine*.2007; 48: 1692-1698
- [3] L. Eriksson, C.C. Watson, K. Wienhard, M. Eriksson, M.E. Casey, C. Knoesa, M. Lenox, Z. Burbar, M. Conti, B. Bandrien, W. D. Heiss and R. Nutt, "The ECAT HRRT: An example of NEMA scatter estimation issues for LSO-based PET systems", *IEEE Transactions on Nuclear Science*, vol. 52, pp 90-94, 2005
- [4] C. C. Watson, M. E. Casey, L. Eriksson, T. Mulnix, D. Adams and B. Bendriem, "NEMA NU 2 performance tests for scanners with intrinsic radioactivity", *Journal of Nuclear Medicine*, vol. 45, pp 822-6, 2004
- [5] S. Yamamoto, H. Horii, M. Hurutani, K. Matsumoto and M. Senda, "Investigation of single, random and true counts from natural radioactivity in LSO-based clinical PET", *Ann Nucl Med* vol. 19, pp. 109-14, 2005.
- [6] S. Jan et al. "GATE: a simulation toolkit for PET and SPECT", *Phys. Med. Biol.* 49 (2004) 4543-4561
- [7] N. Karakatsanis, N. Sakellios, N.X. Tsantillas, N. Dikaios, C. Tsoumpas, D. Lazaro, G. Loudos, C.R. Schmidtlein, K. Louizi, J. Valais, D. Nikolopoulos, J. Malamitsi, J. Kandarakis and K. Nikita, "Comparative evaluation of two commercial PET scanners, ECAT EXACT HR+ and Biograph 2, using GATE", *Nuclear Instruments and Methods in Physics Research, Section A*, Vol. 569, Issue 2, pp 368-372, 2006
- [8] P. Gonias, N. Bertsekas, N. Karakatsanis, G. Saatsakis, A. Gaitanis, D. Nikolopoulos, G. Loudos, L. Pappaspyrou, N. Sakellios, X. Tsantillas, A. Daskalakis, P. Liaparinis, K. Nikita, A. Louizi, D. Cavouras, I. Kandarakis and G.S. Panayiotakis, "Validation of a GATE model for the simulation of the Siemens biograph 6 PET scanner", *Nuclear Instruments and Methods in Physics Research Section A*, Vol. 571, Issues 1-2, pp 263-266, 2007
- [9] N. Karakatsanis, Q. Bao, N. Vu and A. F. Chatziioannou, "Investigation of the minimum detectable activity level of a preclinical LSO PET scanner", *IEEE Nuclear Science Symposium Conference Record*, 2007, Oct. 26th 2007, Vol. 4, Pages 3133-3138
- [10] K. Thielemans, D. Sauge, C. Labbe, C. Morel, M. Jacobsen and A. Zverovich, "STIR Software for Tomographic Image Reconstruction: User's Guide, Version 1.3 Hammersmith Imanet, 2004", <http://stir/irsl.org/documentation/STIR-UsersGuide.pdf>